Machine Learning-Enhanced Gyro mmID-Sensor for Virtual Reality and Motion Tracking Applications

Marvin Joshi[#1], Charles Lynch[#], Genaro Soto-Valle[#], Ajibayo Adeyeye[#], Ryan Bahr[*], Manos Tentzeris[#]
[#]ATHENA Lab, Georgia Institute of Technology, USA
[*]Nano Dimension, USA
[1]mjoshi5@gatech.edu

***Abstract*— The development of virtual reality (VR) and augmented reality (AR) technologies has drawn great attention in recent times due to the wide variety of applications they can enable, spanning from surgery training to motion capture and everyday users in VR spaces. In order to further enhance the user experience, real-time and accurate orientation detection of the user, the authors propose the usage of a Frequency-Modulated Continuous-Wave (FMCW) radar system with an ultra-low-power, sticker-like mmID that is comprised of four backscattering elements that are multiplexed in amplitude, frequency, and spatial domains in order to train a supervised learning KNN-model for accurate real-time 3-axis orientation detection. The proposed orientation detection system achieves a very good (91.72%) accuracy over three axes at 7 m, highlighting the precise orientation detection of the system for medium-range VR/AR applications.**

***Keywords*— millimeter-Wave, RFID, Machine Learning, Radar, AR/VR**

I. Introduction

In recent years, technical advancement has allowed for virtual reality (VR) and augmented reality (AR) to be used for many applications. With its emergence in healthcare, automotive industry and the metaverse, the interest in VR and AR will only rise. In these fields, the ability to detect, localize, and determine the orientation of a target is critical for providing an immersive experience for the user.

A popular way to perform localization is the use of Radio Frequency Identification (RFID) technology. Due to its low manufacturing costs and ultra-low-power consumption, RFID tags have been commonly used for applications involving sensing, motion tracking, and localization. With the emergence of millimeter-wave (mm-Wave) readers, RFID technology can be extended to higher frequencies in the form of Millimeter-Wave Identification (mmID) tags. Due to the available bandwidth alloted by the Federal Communications Commission (FCC) and the high frequency of operation, these mmIDs-based systems inherently benefit from increased ranging accuracy and compact, wearable form-factors, crucial for VR/AR applications. Recent works have achieved highly accurate localization estimations by means of a Frequency-Modulated Continuous-Wave (FMCW) reader [1], [2]. While location detection is important in VR/AR, the ability to detect precise object orientation is just as vital. The orientation of an object can be defined by the roll, yaw, and pitch axes of rotation in a three-dimensional space, as denoted in Fig. 1.

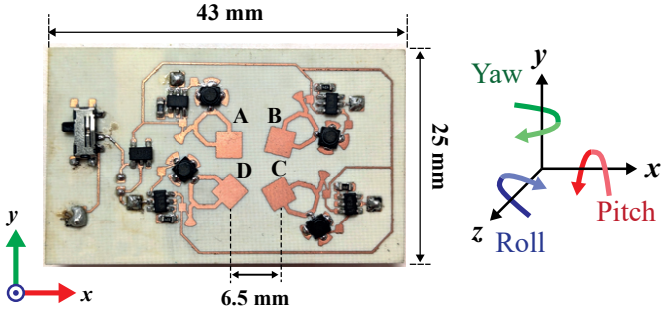

Fig. 1. Proof-of-concept 24 GHz Gyro mmID tag and diagram of rotational movements for each axis.

Various techniques have been used in previous works displaying the use of RFID tags for orientation tracking. Single-axis orientation detection has been shown at low frequencies in [3], [4], [5]. These systems however are both large in size along and have limited reading range. Machine learning has shown to improve results in these single-dimension applications, as high accuracy was achieved in [6]. In [7], [8], the authors demonstrated the ability to detect orientation estimation in multiple axes with the use of multiple tags. While limited in reading range due to low operational frequency, the large form factor of the tags along with low detection accuracy limits these systems. In this work, the authors propose the use of an ultra-low-cost, compact, wearable mmID system combined with machine learning to accurately predict the 3-axis orientation of a mmID-tag for virtual reality and motion tracking applications.

II. Low Cost mm-Wave System

A. *Ultra-low-power Gyro Tag*

The mmID tag used was designed to operate at 24.125 GHz and consists of two sections: the RF front end and the baseband circuit. An RF front end design, similar to [6], for three-axes orientation-detecting mmID was chosen. The design is composed of four distributed cross-polarized antenna elements, each with a modulating loading made from a super low noise amplifier FET (CE3520K3 from CEL) with radial stubs. While only 3 elements are needed to track orientation, as demonstrated in [8], a fourth antenna was used for reliability and to allow for a finer encoding in amplitude along the roll axis. Fig. 1 shows the layout of the tag, where elements A-D

have a modulating frequency of 49 kHz, 69 kHz, 85 kHz and 110 kHz, respectively. Modulation frequencies were chosen to avoid harmonic interference and kept $< 3^{rd}$ harmonic of each other. Additionally, reducing the modulation frequency of each element allows for the mmID tag to have low power consumption. Cross polarization configuration was utilized for each antenna to reduce interference from received signals to the reader. Each antenna was designed to have a polarization offset of 15° from each other. This was done to encode Roll angle of rotation information on the relative received amplitude of each element whereas the relative phase difference between two elements will be minimal with a rotation in the Roll axis. The baseband circuit is used to generate the modulating signal for each element. Here, the resistor set voltage-controlled oscillator (VCO) LTC6906 is used for its low power and ability to control the generated frequency. A 1.8 V voltage regulator is used to provide voltage to the VCO in order to guarantee consistent performance. To power the board, a 3 V coin cell battery is used. The mmID was designed on Rogers RO4350B (ϵ_r = 3.66, $\tan\delta$= 0.0037), with antenna elements spaced by 6.5 mm, which corresponds to $\approx \frac{\lambda}{2}$.

B. FMCW Reader

The Analog Devices EV-RADAR-MMIC2 Evaluation Board, an 24 GHz FMCW radar, was used as the proof-of-concept reader for the three axis orientation detection Gryo tag. This board is made up of the ADF5901 24 GHz monolithic microwave integrated circuit (MMIC) transmitter, ADF5904 24 GHz MMIC receiver, and the ADF4159 13 GHz phase-locked loop (PLL). The A-INFO LB-180400-20-C-KF horn antennas, which provide 20 dBi of gain, were used for both the transmitter and receiver in a cross-polarized configuration. A 40 dB Low Noise Amplifier (LNA) with a noise figure (NF) of 3.2 dB was used on the receiving antenna to improve the system's sensitivity. The radar was configured to a triangular chirp waveform, with a frequency slope of 400 $\frac{\text{MHz}}{\mu\text{s}}$ and a chirp period of 5 ms.

III. Signal Processing

A. Range FFT and Phase Extraction

Fig. 2 shows the block diagram of the proposed signal processing scheme. A Fast Fourier Transform (FFT) is performed on the received signal of each positive slope and negative slope ramp to visualize the magnitude spectrum. From this spectrum, the modulating beat frequencies of each element on the tag can be extracted. An example spectrum can be found in Fig. 3. Here, the negative and positive modulating peaks of each element can be seen, centered at their corresponding modulation frequency.

Once the range FFT is performed, a custom peak detection algorithm is used to identify the modulating beat frequencies of each element. From these frequencies, the phase difference of elements B-A, C-B, D-C and A-D can be determined. Phase difference of received signals play an important roll at farther reading ranges. As the signal strength from each element attenuates with an increase in the range from

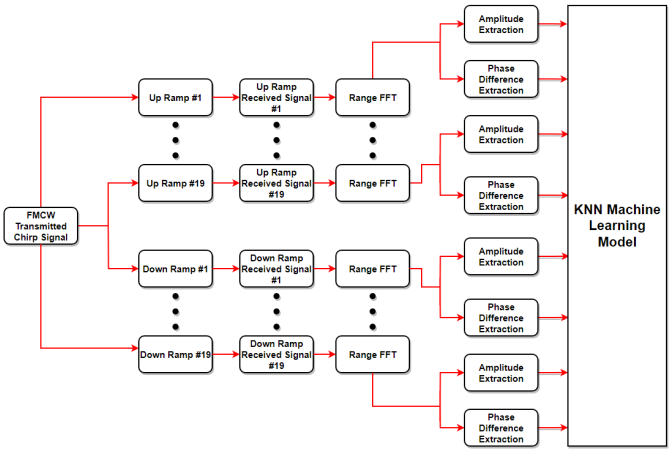

Fig. 2. Signal Processing Chain to Extract Amplitude and Phase Response of the Tag.

the reader-consequently reducing the dynamic range of the amplitude response with respect rotation- the phase has been shown to be more reliable [9]. Arctangent Demodulation is a method used to extract the phase of I/Q Signals over a range profile. This algorithm determines the phase angle of the radar signal and uses phase unwrapping to prevent any phase drift larger than $\pm\pi$ [10]. This is done by adding $\pm 2\pi$ to the extracted phase if phase drift is found to occur. Therefore, by extracting the relative phase differential between each element on the Gyro mmID and in turn forming a higher dimensional training set with respect to three-axis rotation, complex orientation estimation with high classification accuracy at medium to long ranges from the radar is enabled.

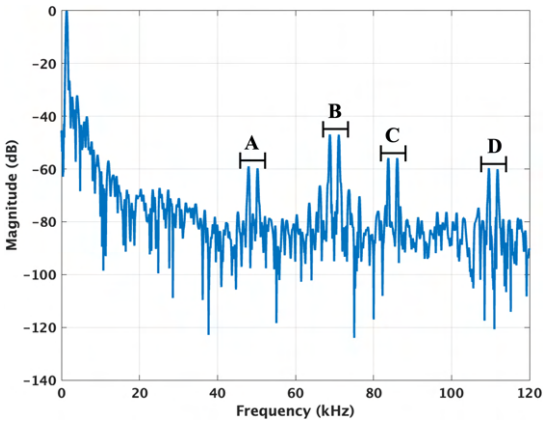

Fig. 3. Proof-of-concept mmID Tag Modulation at Broadside.

B. Machine Learning

The K-Nearest Neighbors (KNN) machine learning algorithm is used for this work. KNN networks are used for classification-based problems in which pattern recognition is performed to find the K-closest values to the prediction. Using the KNN algorithm, two models were trained. The first model, Model A, uses only the amplitude response from each element on the tag with respect to orientation. The second model,

Model B, includes the phase difference from neighboring antennas, i.e. elements B-A, C-B, D-C and A-D, along with the amplitude response from each element with respect to orientation. For each experiment, each feature was scaled using min-max normalization.

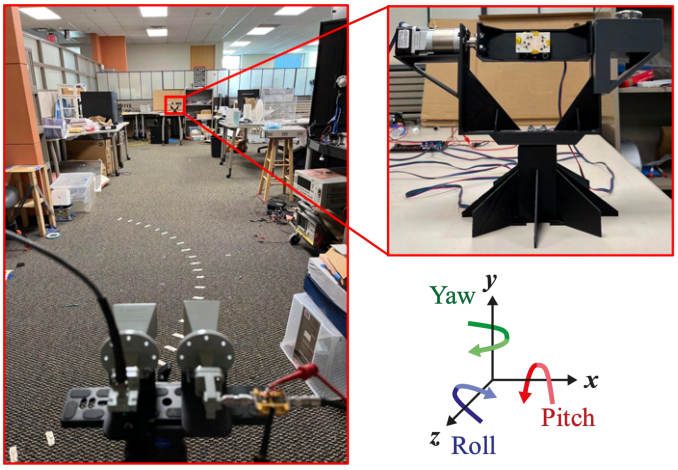

Fig. 4. Experimental Setup at 10 m.

IV. Experimental Validation

A. Experimental Setup

The experimental setup used can be found in Fig. 4. To rotate along all three axes, the tag was mounted onto a 3-Axis Gimbal holder. For precise angular steps, each axis was individually controlled by a planetary geared stepper motor. Each motor was swept over a $\pm$ 90° range with increments of 10°, which results in 6859 different orientations of the tag. This range was chosen as it allows for complete coverage in the angular space in which a tag can be detected. To display the transmitted and received signal, the Tektronix DPO 7354 Oscilloscope was used. The oscilloscope was set to a sampling rate of 500 kHz with 19 up and down ramps recorded resulting in 38 total observations per angular configuration, which gives a total of 260,642 unique samples. Additionally, a synchronized clock was also used to sync the radar with the oscilloscope to for timing purposes to ensure proper acquisition of the relative phase differential between elements.

B. Measurements and Results

Experiments were performed at 11 different distances, 0.5m, 1m, 2m, 3m, 4m, 5m, 6m, 7m, 8m, 9m, and 10m. A global set was then formed by combining the data from each experiment, which results in a dataset of 2,867,042 samples. Due to the large size of the dataset, a train-test split of 80/20 was used, where 80% of the data was for training the model, while the other 20% to test its performance. The results for both models can be found in Table 1. From this table, it can be seen that the addition of phase greatly improves accuracy at farther distances, as the accuracy of Model B was more than 2x that of Model A. It can also be seen that for both models, as the range increases, the model becomes less accurate.

Table 1. Comparison of KNN Models trained with and without Phase Difference.

Range	Model A	Model B	Model B with 70/30 Split
0.5 m	99.60%	99.91%	99.83 %
1 m	95.59%	99.88%	99.82 %
2 m	81.19%	99.63%	99.80 %
3 m	67.29%	99.12%	98.63 %
4 m	58.81%	97.48%	97.83 %
5 m	53.29%	95.63%	93.27 %
6 m	47.14%	93.48%	90.98 %
7 m	46.45%	91.72%	85.91 %
8 m	41.89%	88.47%	79.64 %
9 m	37.36%	84.25%	76.85 %
10 m	35.54%	81.64%	68.60 %

Model B was also retrained with a 70/30 train-test split, to observe the effect of training with a compressed data set. The results from this updated model can be seen in Table 1. While similar results were obtained up to 6 m, the accuracy greatly deteriorates at longer distances.

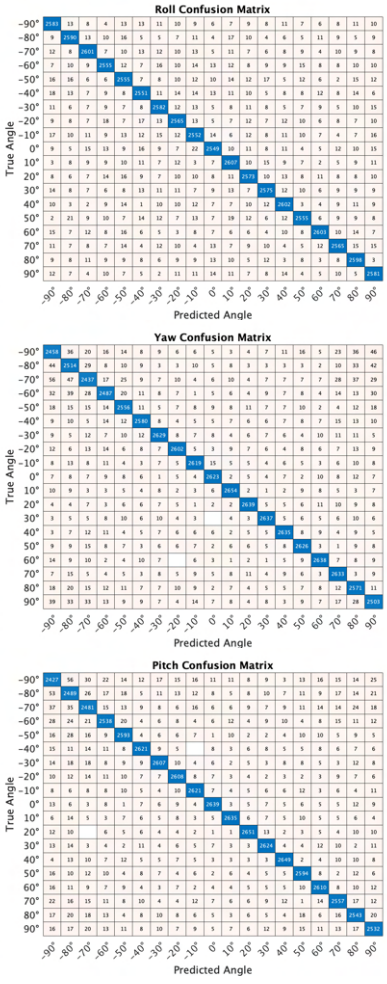

Fig. 5. Confusion Matrices at 4 m: (a) Roll Axis Fixed with Yaw and Pitch Axes Rotating, (b) Yaw Axis Fixed with Roll and Pitch Axes Rotating, (c) Pitch Axis Fixed with Roll and Yaw Axes Rotating.

Fig. 5 shows the confusion matrices for all three axes at $4\,\mathrm{m}$ using Model B. Each matrix is a combination of all rotations while one axis is locked at a set angle and the other two are rotating from $\pm$ 90°. For example, the Yaw Confusion Matrix at 90° is a combination of all rotations of pitch and roll, while the yaw axis is set at 90°. It can be seen for all three axis, false estimations tend to occur when the angle is beyond $\pm$ 60°. Similar trends were found in the other experiments, which are likely the result of the tag no longer being within the beamwidth of the transmitting and receiving antenna.

Additional tests were performed at each distance to validate Model B. The tag was rotated in 14 different paths, which resulted in 245 different orientations. Fig, 6 shows the results when the tag is at a range of $4\,\mathrm{m}$. This plot clearly shows that Model B was able to accurately classify the orientation of the tag, as an accuracy of 97.12% was obtained, which follows the testing results shown in Table 1.

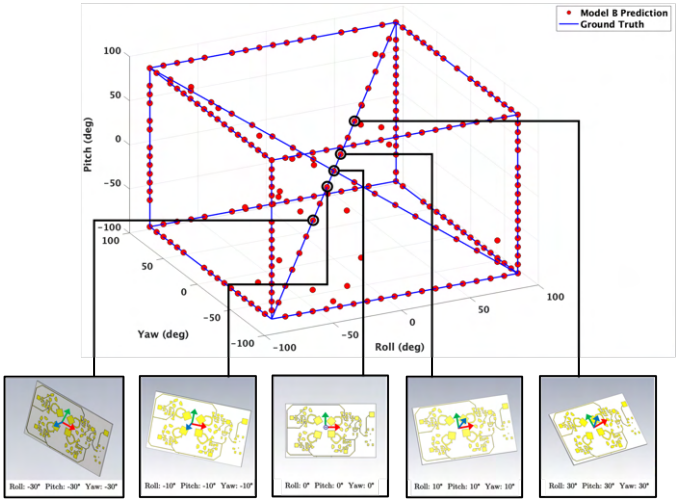

Fig. 6. Predicted Orientation vs Real Orientation at Range = $4\,\mathrm{m}$.

V. Conclusion

In this work, the authors proposed the use of a highly scalable, ultra-low power FMCW reader with a $24\,\mathrm{GHz}$ mmID tag to predict its 3-axis orientation using a KNN machine learning algorithm at long range. Two models were tested in which the benefit of tracking the phase difference of neighboring antenna elements was demonstrated. Additionally, the proposed system features an accuracy of >91% even at a range of $7\,\mathrm{m}$ from the proof-of-concept reader. Further evaluation of the proposed system will be explored with a finer angular resolution for an even more precise orientation detection. With VR/AR applications requiring low latency and devices capable of highly accurate orientation tracking to allow for an immersive experience, the proposed low-cost mmID tag is a prime candidate for future systems that require the mapping of AR objects into the user experience. Moreover, the advance of wireless motion capture systems can greatly benefit from the proof-of-concept mmID sensor presented in this paper, by integrating multiple mmID tags where each of them can provide accurate location and orientation information, thus lowering the overall costs and avoiding the need for expensive optical camera configurations.

References

[1] C. A. Lynch, A. O. Adeyeye, J. G. Hester, and M. M. Tentzeris, "When a single chip becomes the rfid reader: An ultra-low-cost 60 ghz reader and mmid system for ultra-accurate 2d microlocalization," in *2021 IEEE International Conference on RFID (RFID)*, 2021, pp. 1–8.

[2] A. Strobel, C. Carlowitz, R. Wolf, F. Ellinger, and M. Vossiek, "A millimeter-wave low-power active backscatter tag for fmcw radar systems," *IEEE Transactions on Microwave Theory and Techniques*, vol. 61, no. 5, pp. 1964–1972, 2013.

[3] G. Gupta, B. P. Singh, A. Bal, D. Kedia, and A. R. Harish, "Orientation detection using passive uhf rfid technology [education column]," *IEEE Antennas and Propagation Magazine*, vol. 56, no. 6, pp. 221–237, 2014.

[4] S. Genovesi, F. Costa, M. Borgese, F. A. Dicandia, A. Monorchio, and G. Manara, "Chipless rfid sensor for rotation monitoring," in *2017 IEEE International Conference on RFID Technology Application (RFID-TA)*, 2017, pp. 233–236.

[5] N. Barbot, O. Rance, and E. Perret, "Cross-polarization chipless tag for orientation sensing," in *2020 50th European Microwave Conference (EuMC)*, 2021, pp. 1119–1122.

[6] A. Adeyeye, C. Lynch, J. Hester, and M. Tentzeris, "A machine learning enabled mmwave rfid for rotational sensing in human gesture recognition and motion capture applications," in *2022 IEEE/MTT-S International Microwave Symposium - IMS 2022*, 2022, pp. 137–140.

[7] Z. Wang, M. Xu, and F. Xiao, "Recognizing 3d orientation of a two-rfid-tag labeled object in multipath environments using deep transfer learning," in *2021 IEEE 41st International Conference on Distributed Computing Systems (ICDCS)*, 2021, pp. 652–662.

[8] M. B. Akbar, C. Qi, M. Alhassoun, and G. D. Durgin, "Orientation sensing using backscattered phase from multi-antenna tag at 5.8 ghz," in *2016 IEEE International Conference on RFID (RFID)*, 2016, pp. 1–8.

[9] C. Hekimian-Williams, B. Grant, X. Liu, Z. Zhang, and P. Kumar, "Accurate localization of rfid tags using phase difference," in *2010 IEEE International Conference on RFID (IEEE RFID 2010)*, 2010, pp. 89–96.

[10] B.-K. Park, O. Boric-Lubecke, and V. M. Lubecke, "Arctangent demodulation with dc offset compensation in quadrature doppler radar receiver systems," *IEEE Transactions on Microwave Theory and Techniques*, vol. 55, no. 5, pp. 1073–1079, 2007.